^{64}Cu-SARTATE PET Imaging of Patients with Neuroendocrine Tumors Demonstrates High Tumor Uptake and Retention, Potentially Allowing Prospective Dosimetry for Peptide Receptor Radionuclide Therapy

Rodney J. Hicks[1,2], Price Jackson[1], Grace Kong[1], Robert E. Ware[1], Michael S. Hofman[1,2], David A. Pattison[1], Timothy A. Akhurst[1], Elizabeth Drummond[1], Peter Roselt[1], Jason Callahan[1], Roger Price[3], Charmaine M. Jeffery[3], Emily Hong[1], Wayne Noonan[4], Alan Herschtal[5], Lauren J. Hicks[6], Amos Hedt[7], Matthew Harris[7], Brett M. Paterson[8], and Paul S. Donnelly[9]

[1]Cancer Imaging, Peter MacCallum Cancer Centre, Melbourne, Victoria, Australia; [2]Sir Peter MacCallum Department of Oncology, University of Melbourne, Parkville, Victoria, Australia; [3]Medical Technology and Physics, Sir Charles Gairdner Hospital, Nedlands, Washington, Australia; [4]Liverpool Hospital, Liverpool, New South Wales, Australia; [5]Biostatistics and Clinical Trials, Peter MacCallum Cancer Centre, Melbourne, Victoria, Australia; [6]Mercy Hospital for Women, Heidelberg, Victoria, Australia; [7]Clarity Pharmaceuticals Ltd., Eveleigh, New South Wales, Australia; [8]School of Chemistry, Monash University, Victoria, Australia; and [9]School of Chemistry and Bio21 Molecular Science and Biotechnology Institute, University of Melbourne, Parkville, Victoria, Australia

Imaging of somatostatin receptor expression is an established technique for staging of neuroendocrine neoplasia and determining the suitability of patients for peptide receptor radionuclide therapy. PET/CT using ^{68}Ga-labeled somatostatin analogs is superior to earlier agents, but the rapid physical decay of the radionuclide poses logistic and regulatory challenges. ^{64}Cu has attractive physical characteristics for imaging and provides a diagnostic partner for the therapeutic radionuclide ^{67}Cu. Based on promising preclinical studies, we have performed a first-time-in-humans trial of ^{64}Cu-MeCOSar-Tyr^3-octreotate (^{64}Cu-SARTATE) to assess its safety and ability to localize disease at early and late imaging time-points. **Methods:** In a prospective trial, 10 patients with known neuroendocrine neoplasia and positive for uptake on ^{68}Ga-DOTA-octreotate (^{68}Ga-DOTATATE) PET/CT underwent serial PET/CT imaging at 30 min, 1 h, 4 h, and 24 h after injection of ^{64}Cu-SARTATE. Adverse reactions were recorded, and laboratory testing was performed during infusion and at 1 and 7 d after imaging. Images were analyzed for lesion and normal-organ uptake and clearance to assess lesion contrast and perform dosimetry estimates. **Results:** ^{64}Cu-SARTATE was well tolerated during infusion and throughout the study, with 3 patients experiencing mild infusion-related events. High lesion uptake and retention were observed at all imaging time-points. There was progressive hepatic clearance over time, providing the highest lesion-to-liver contrast at 24 h. Image quality remained high at this time. Comparison of ^{64}Cu-SARTATE PET/CT obtained at 4 h to ^{68}Ga-DOTATATE PET/CT obtained at 1 h indicated comparable or superior lesion detection in all patients, especially in the liver. As expected, the highest early physiologic organ uptake was in the kidneys, liver, and spleen. **Conclusion:** ^{64}Cu-SARTATE is safe and has excellent imaging characteristics. High late-retention in tumor and clearance from the liver suggest suitability for diagnostic studies and for prospective dosimetry for ^{67}Cu-SARTATE peptide receptor radionuclide therapy, and the half-life of ^{64}Cu would also facilitate good-manufacturing-practice production and distribution to sites without access to ^{68}Ga.

Key Words: radiopharmaceuticals; copper-64; neuroendocrine tumor; peptide receptor radionuclide therapy; positron emission tomography; theranostics

J Nucl Med 2019; 60:777–785
DOI: 10.2967/jnumed.118.217745

PET/CT using ^{68}Ga-DOTA-octreotate (^{68}Ga-DOTATATE), marketed commercially as NETSPOT (Advanced Accelerator Applications) or other ^{68}Ga-labeled somatostatin analogs (SSAs), is becoming the gold standard for neuroendocrine neoplasia (NEN) diagnosis and staging (*1*). ^{68}Ga-DOTATATE is particularly important in determining the suitability of patients for peptide receptor radionuclide therapy (PRRT) (*2,3*). By virtue of its higher sensitivity for NEN than conventional imaging techniques, including ^{111}In-pentetreotide (OctreoScan; Mallinckrodt Pharmaceuticals) SPECT/CT, ^{68}Ga-DOTATATE PET/CT has been shown to have a significant impact on patient management decisions (*4*). The efficacy and safety of PRRT depends on delivering the highest possible dose to the tumor deposits while sparing organs, particularly the kidneys, from radiation toxicity (*5–7*). Although quantitative SPECT/CT techniques can provide verification of the radiation dose delivered from each cycle of PRRT (*8*), ideally, dose estimation should be performed before therapeutic administration. Accurate prospective dosimetry would allow prescription of an administered activity that maximizes therapeutic efficacy within the tolerance of normal tissues. In the absence of such information, most facilities providing PRRT administer a standardized activity of 7–8 GBq of ^{177}Lu-labeled SSA or 2–4 GBq of ^{90}Y-labeled SSA. This strategy

Received Aug. 1, 2018; revision accepted Nov. 1, 2018.
For correspondence contact: Rodney J. Hicks, Peter MacCallum Cancer Centre, Cancer Imaging, Level 5, 305 Grattan St., Melbourne VIC 3000, Australia.
E-mail: rod.hicks@petermac.org
Published online Nov. 15, 2018.

has generally been successful in providing moderate response rates with low toxicity as well as median progression-free and overall survival durations that have been encouraging both in single-center studies (*9*) and in the only randomized control trial performed to date, the NETTER-1 trial of ^{177}Lu-DOTATATE versus dose-escalated SSA therapy (*10*). However, we believe that the therapeutic index may be further improved by an individualized rather than an empiric approach (*11*). Because of the so-called sink effect, changes in the burden of disease and tumor avidity as treatment progresses can lead to marked variability in radiation delivery to both lesions and normal organs (*12*). The quantitative capability of PET/CT provides the opportunity to assess uptake and retention of radioactive peptides in tumor and normal tissues and, thereby, to provide truly individualized prospective dosimetry. This capability was first demonstrated using ^{86}Y-SSA PET before ^{90}Y-SSA PRRT (*13*). Although ^{68}Ga has been widely used as the diagnostic pair of ^{177}Lu, it has a half-life of only 68 min, which is insufficiently long to model the retention and clearance kinetics required for accurate dosimetry estimation in individual patients. This is particularly the case for organs with significant clearance over time, which include the kidneys and liver. Of longer-lived positron-emitting radioisotopes, the physical half-life of ^{64}Cu (12.7 h) provides an opportunity to assess the clearance kinetics out to, and potentially beyond, 24 h after tracer administration. This could also provide a diagnostic pair both to assess suitability of patients for ^{67}Cu PRRT and to enable predictive dosimetry. ^{67}Cu is a β-emitting radionuclide with favorable physical characteristics for therapeutic application (*14*).

Our group has recently reported the synthesis and preclinical evaluation of ^{64}Cu-MeCOSar-Tyr^3-octreotate (^{64}Cu-SARTATE) (*15*) based on a cage amine ligand called sarcophagine (Sar). An advantage of the MeCOSar, when compared with DOTA, is that copper (II) sarcophagine complexes are more stable than copper (II) DOTA complexes. In a murine xenograft model, the uptake of ^{64}Cu-SARTATE in somatostatin receptor–expressing tumors after 2 h was high, at 63.0 ± 15.0 percentage injected dose (%ID)/g, and remained high after 24 h, at 105 ± 27.1 %ID/g. This high retention at late time-points suggests superior potential for personalized PRRT dosimetry planning and therapeutic application. Accordingly, we have performed a single-center open-label, phase 0–1 investigation of ^{64}Cu-SARTATE in patients with World Health Organization grade 1 or 2 NEN. Our hypotheses were that ^{64}Cu-SARTATE can be safely administered to humans and will facilitate identification of somatostatin receptor–expressing tissues using PET/CT scanning, with absorbed radiation doses that are appropriate for clinical use but with sufficient late retention to enable prospective radiation dosimetry.

MATERIALS AND METHODS

The trial protocol was approved by our institutional ethics committee as a first-time-in-humans study and was registered with the Therapeutic Goods Administration as an Australian Clinical Trial Notification (2015/0320). All patients provided written informed consent. The study was pragmatically designed to include up to 10 participants. Interim safety analyses were planned after 1, 2, and 5 study subjects had completed all required investigations. The trial flow-chart is displayed in Figure 1.

The primary objectives of this study were to estimate the rate of occurrence of adverse clinical, biochemical, or hematologic events after ^{64}Cu-SARTATE administration; the %ID and SUVs of ^{64}Cu-SARTATE found in organs of interest at early and late time-points after administration of the investigational product; and absorbed organ doses (expressed as μGy/MBq of administered ^{64}Cu-SARTATE) and whole-body dose (expressed as mSv/200 MBq of administered activity).

The secondary objectives of this study were to determine whether ^{64}Cu-SARTATE PET/CT scans at 1, 4, and 24 h demonstrate known sites of malignancy with tumor-to-background ratios that are equivalent to, or greater than, those achieved using routine clinical ^{68}Ga-DOTATATE acquisitions at 1 h, thereby enabling same-day diagnostic evaluation, and, if tracer is retained in lesions on the day after administration, to support its use for prospective radiation dosimetry calculations as an aid in the development of ^{67}Cu-SARTATE as a therapeutic agent. Reporting clinician preference for image quality was also assessed.

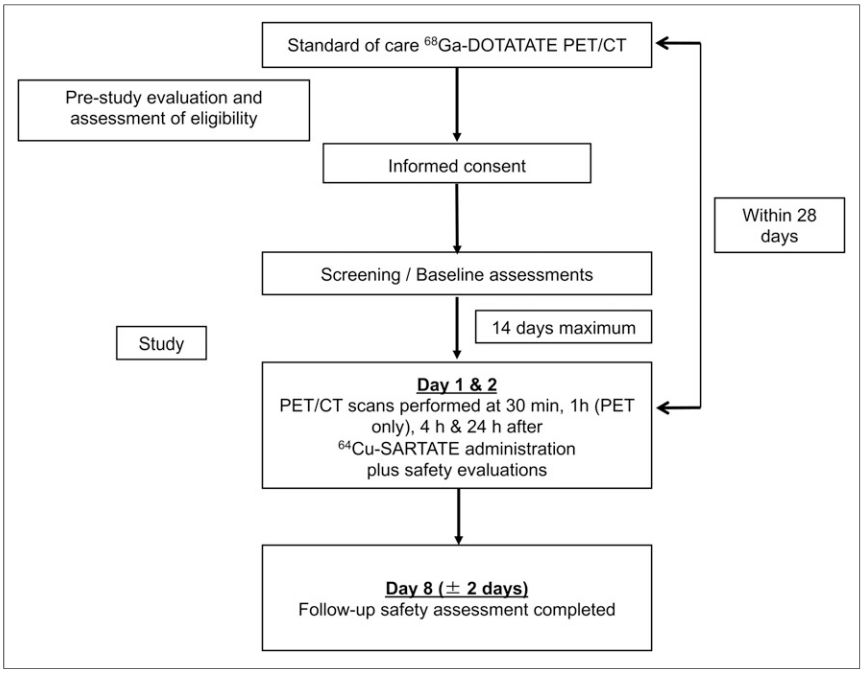

FIGURE 1. Study flow chart.

Eligibility criteria were as follows: signed informed consent; an age of 18 y or older; life expectancy of at least 8 wk; biopsy-proven World Health Organization G1 or G2 (Ki-67 index, 0%–2% and 3%–20%, respectively) NEN; at least 1 site of active somatostatin receptor–positive malignancy, as demonstrated on ^{68}Ga-DOTATATE PET/CT scanning performed as part of routine clinical care; a creatinine clearance of more than 60 mL/min as estimated by the Cockcroft–Gault formula (using actual body weight); and Eastern Cooperative Oncology Group performance of 0–2.

The exclusion criteria were pregnancy or breastfeeding; known sensitivity or allergy to SSAs; interventional treatment received for NEN in the interval between ^{68}Ga-DOTATATE PET/CT and ^{64}Cu-SARTATE PET/CT scanning; treatment with long-acting SSAs within 28 d before test agent administration; treatment with short-acting SSAs within 24 h before test agent administration; a QTc interval

TABLE 1
Baseline Characteristics

Variable	Statistic/level	Count/value
Sex (*n*)	F	4
	M	6
Age (y)	Mean	63.2 (SD, 10)
	Median	62 (range, 46–78)
	Interquartile range	57.2–71.5
Baseline ECOG	0	6 (60%)
	1	4 (40%)
Baseline EGFR	≤70	3 (30%)
	>70	7 (70%)
Weight (kg)	Mean	87.7 (SD, 16)
	Median	90.5 (range, 60–112)
	Interquartile range	74.6–98
Height (cm)	Mean	173.2 (SD, 7)
	Median	173 (range, 163–185)
	Interquartile range	168–176.5

ECOG = Eastern Cooperative Oncology Group performance; EGFR = estimated glomerular filtration rate (mL/min/1.73 m²).

of more than 0.44 s as measured by screening electrocardiography; any serious medical condition that the investigator felt may interfere with the procedures or evaluations of the study; unwillingness or inability to comply with the protocol or a history of noncompliance; and inability to grant informed consent.

Safety Analysis

Safety evaluations were performed 1 d and 1 wk after tracer administration. These included physical examination, full blood examination, urea and electrolytes, liver function tests, and electrocardiography. Patient-reported adverse events were recorded during administration of the radiotracer and after each scan and reported using the Common Terminology Criteria for Adverse Events, version 4.0, as published by the National Cancer Institute.

PET/CT

The PET/CT scans were acquired on a Discovery 690 scanner (GE Healthcare), which has time-of-flight acquisition and a 64-slice CT scanner. CT scans were performed from the vertex to the lower thighs for the purposes of attenuation correction, localization of lesions, and estimation of tumor volumes. These findings were correlated with recent contrast-enhanced CT when available. A low-dose, unenhanced technique was used (140 kVp, 40–200 mAs, GE Healthcare SmartmA), with a final reconstructed slice thickness of 3.27 mm. Our standard ^{68}Ga-DOTATATE PET/CT acquisition protocol was used. This involves a weight-based, intravenous administration of 150–300 MBq of radiopeptide with acquisition of 6–8 bed positions (3 min per bed position). PET scans were reconstructed using the ordered-subset estimation method with 2 iterations and 20 subsets with a 3.25-mm filter in a 128 × 128 matrix over a 55-mm reconstructed transaxial field of view.

^{64}Cu-SARTATE was prepared using a modified version of a previously described method (*15*). Briefly, ^{64}Cu(II) (500–800 MBq, 0.02 M HCl) was added to SARTATE (20 μg) in a solution of 4% ethanol in 0.1 M ammonium acetate and a 1 mg/mL solution of gentisic acid, sodium salt (5 mL). The reaction mixture was incubated for 30 min at room temperature and then passed through a Strata-X (Phenomenex, Inc.) cartridge (30 mg). Cartridge-retained ^{64}Cu-SARTATE was rinsed with saline for injection before elution with ethanol into a vial containing saline for injection. The contents of this vial

TABLE 2
Mean and SD of ^{64}Cu-SARTATE %ID for Normal Organs

Organ	30 minutes	1 hour	4 hours	24 hours
Adrenals	0.19 (0.13)	0.17 (0.12)	0.19 (0.14)	0.17 (0.16)
Brain	0.23 (0.06)	0.17 (0.10)	0.22 (0.06)	0.16 (0.06)
Lower large intestine	0.42 (0.18)	0.44 (0.21)	0.47 (0.19)	0.69 (0.37)
Small intestine	4.40 (1.38)	4.32 (0.99)	3.78 (1.37)	2.90 (0.83)
Stomach	1.69 (1.26)	1.73 (1.22)	0.68 (0.87)	0.82 (0.61)
Upper large intestine	1.60 (1.59)	1.77 (1.65)	1.44 (1.19)	1.34 (0.59)
Heart	0.76 (0.37)	0.66 (0.31)	0.48 (0.30)	0.37 (0.19)
Kidneys	6.40 (1.59)	5.22 (1.51)	4.33 (0.91)	3.49 (0.68)
Liver	15.02 (2.06)	13.90 (2.30)	11.79 (3.12)	6.79 (2.87)
Lungs	0.99 (0.18)	0.90 (0.25)	0.66 (0.18)	0.46 (0.12)
Muscle	2.27 (0.48)	2.13 (0.44)	1.82 (0.51)	1.32 (0.36)
Pancreas	0.52 (0.25)	0.49 (0.31)	0.50 (0.39)	0.41 (0.24)
Red marrow	7.15 (1.39)	6.28 (1.39)	5.62 (1.38)	4.44 (0.99)
Spleen	4.68 (1.90)	4.94 (1.96)	5.41 (2.07)	4.06 (1.90)
Thyroid	0.05 (0.02)	0.04 (0.02)	0.04 (0.02)	0.04 (0.03)
Urinary bladder	5.27 (3.55)	5.72 (4.71)	2.13 (2.85)	1.49 (1.11)
Remainder of body	55.62 (11.63)	56.77 (12.44)	52.58 (14.02)	42.34 (13.45)

SDs are in parentheses.

were filtered through a 0.22-μM filter. ^{64}Cu-SARTATE was recovered in 60%–80% radiochemical yield with more than 95% radiochemical purity. The average peptide mass administered was 6.4 ± 4.7 μg (range, 3.6–19.5 μg). After intravenous administration of approximately 200 MBq of ^{64}Cu-SARTATE (mean, 192 ± 24 MBq; range, 125–209 MBq), PET scans were acquired over the same axial extent with 3-dimensional acquisition of 8 bed positions (1.5 min per bed position for the 30- and 60-min scans, 2.0 min for the 240-min scans, and 3 min for the 24-h scan). PET scans were reconstructed with 2 iterations, 18 subsets, and a 7-mm gaussian smoothing kernel to mitigate image noise. All scans were performed at a mean of 14 ± 9 d (range, 6–27 d) of the ^{68}Ga-DOTATATE PET/CT that determined eligibility for the study.

Analysis of ^{64}Cu-SARTATE Scans

Qualitative analysis of each subject's PET/CT scans was performed independently by 2 qualified nuclear medicine physicians masked to the clinical details of the patient. The ^{68}Ga-DOTATATE and ^{64}Cu-SARTATE scans obtained at approximately 1 h were presented side by side in a deidentified manner with the physicians indicating the image quality of each scan on a 5-point scale. They then indicated if any suspected lesions were identified on one scan but not seen on the other. The number and location of such discordant lesions were recorded. After this direct comparison of each scan type at the 1-h time point, the series of 4 individual ^{64}Cu-SARTATE image sets acquired from 30 min to 24 h after injection were displayed in a random order against each other and the ^{68}Ga-DOTATATE images. The physicians

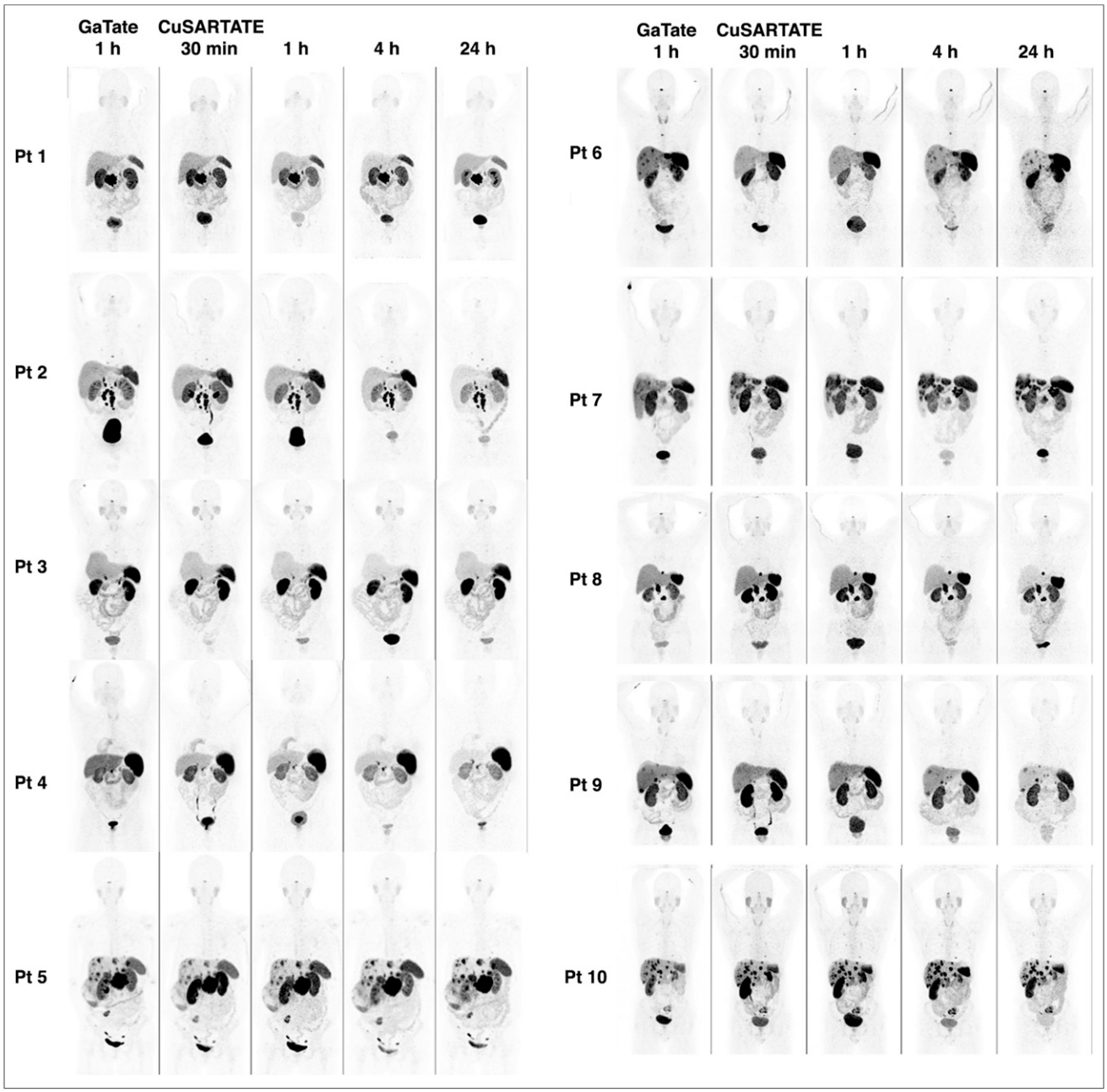

FIGURE 2. Comparison of tracers. Maximum-intensity projections obtained at 1 h for ^{68}Ga-DOTATATE (GaTate) are compared with those obtained at 30 min, 1 h, 4 h, and 24 h for ^{64}Cu-SARTATE. Although ^{64}Cu-SARTATE images were deemed comparable at 1 h in 9 of 10 patients (patient 6 was the exception), all were considered equivalent or superior to ^{68}Ga-DOTATATE at both 4 h and 24 h.

were asked to score image quality for each time point and to indicate whether any lesions were apparent on one scan but not the other.

SUV was estimated for up to 5 reference lesions (with no more than 3 per organ) on ^{68}Ga-DOTATATE obtained at 1 h after injection using volume-of-interest software (MIM Encore; MIM Software Inc.). If able to be identified, the same lesions were analyzed on the ^{64}Cu-SARTATE scans at 1, 4, and 24 h. Further, SUV_{mean} estimations for normal liver, lungs, spleen, kidneys, bone marrow, thyroid, and pituitary gland were also obtained for ^{64}Cu-SARTATE at 1, 4, and 24 h. Lesion-to-liver ratios were calculated for reference deposits at 1, 4, and 24 h to determine the optimal time for detection of hepatic lesions, which are common among patients with metastatic NEN (*16*).

For radiation cross-dose analysis, the source organs considered were the adrenals, brain, upper and lower large intestine contents, small intestine contents, stomach contents, heart contents, kidneys, liver, lungs, muscle, pancreas, red marrow, spleen, thyroid, urinary bladder contents, and the remainder of the body. Organs were contoured on the 30-min PET/CT series, and each subsequent time point was fused by rigid and deformable image registration (*17*). For each contoured region, the mean activity concentration was recorded, and the total region activity was determined on the basis of standard MIRD adult source-organ volumes. Three-phase time–activity curves were generated through an automated routine (*18*), and integrated cumulated activity values (MBq·h/MBq) were converted to organ self- and cross-doses using OLINDA dose factors (S values) (*19*). Mean organ doses, effective dose contribution, and total effective dose were based on International Commission on Radiological Protection Publication 89 tissue-weighting factors.

Statistical Analysis

All statistical analyses were performed in the R statistical software package, version 3.4.2, using standard and validated statistical procedures. All statistical analysis results and their interpretation were independently reviewed by a qualified statistician. The %ID in each organ of interest (liver, lungs, spleen, kidneys, bone marrow, thyroid, pituitary gland) across the 10 patients at each time point are reported using standard descriptive baseline statistics, including means, SD, medians, and ranges for continuously valued variables, and cell counts and percentages for categorically valued variables. Statistical methods consisted of production of Bland–Altman plots and Wilcoxon tests for paired data, performed using the base package of the R language for statistical computing and commonly used add-on packages (gdata, Hmisc, plyr, R2wd, and utils). *P* values of less than 0.05 on paired analyses were considered significant.

RESULTS

In total, 10 patients were recruited between June and October 2015. The clinical characteristics of these patients are included in Table 1.

Safety of ^{64}Cu-SARTATE

No grade 3 or 4 adverse events were reported. A single grade 2 event was recorded (transient wheezing). However, this was considered unrelated to treatment. Five grade 1 events were recorded: 2 were considered unrelated to the investigational agent (nausea and petechial rash), 2 were considered possibly related (flushing and leukopenia), and 1 (lymphopenia) was considered probably related. Except for the 2 hematologic reactions, the adverse events were of short duration (<7 d). The patient with lymphopenia (patient 9) had previously received PRRT and had lymphocyte counts persistently in the lower end of the reference range since treatment. These dipped to 0.95×10^9/L (reference range, $1.00–4.00 \times 10^9$/L) at 1 wk after the scan before returning to the low reference range within 4 wk. The patient with leukopenia (patient 6) had a normal baseline white cell count that dropped to 3.9×10^9/L (reference range, $>4.00 \times 10^9$/L) at 6 wk after the scan before returning to the reference range by follow-up at 3 mo.

%ID and SUV in Reference Organs and Tissues

The %ID in reference tissues and organs are detailed for each imaging time-point in Table 2. As expected, there was relatively rapid clearance of blood-pool activity, slower clearance of renal activity, and intermediate clearance of hepatic activity. High retention was seen in tumor and organs with high somatostatin receptor expression, including the pituitary and spleen.

TABLE 3
Comparison of Lesion and Normal-Organ Uptake and Retention for ^{68}Ga-DOTATATE and ^{64}Cu-SARTATE

Measure	^{68}Ga-DOTATATE	^{64}Cu-SARTATE	Difference	95% CI	*P**
Median at 1 h					
Max lesion SUV_{max}	31.65	41.90	12.45	5.1, 21.4	0.010
Mean patient SUV_{max}	23.61	33.32	10.35	5.4, 15.3	0.002
Liver SUV_{mean}	7.10	7.45	0.30	−0.2, 0.8	0.24
Spleen SUV_{mean}	20.40	28.25	9.05	4.0, 14.9	0.004
Kidney SUV_{mean}	13.10	20.98	6.80	5.4, 12.1	0.002
Median at 1 h (^{68}Ga-DOTATATE) or 4 h (^{64}Cu-SARTATE)					
Max lesion SUV_{max}	31.65	50.50	17.10	9.6, 36.3	0.004
Mean patient SUV_{max}	23.61	34.80	12.99	6.3, 27.9	0.004
Liver SUV_{mean}	7.10	5.90	−1.05	−2.2, 1.0	0.19
Spleen SUV_{mean}	20.40	35.55	17.50	7.7, 102.2	0.020
Kidney SUV_{mean}	13.10	18.05	4.86	2.1, 7.0	0.004

*Paired Wilcoxon test on 10 patients.
CI = confidence interval; max lesion = most intense lesion; mean patient = mean of up to 5 reference lesions.

TABLE 4
Comparison of Lesion-to-Liver Ratios of ^{68}Ga-DOTATATE and ^{64}Cu-SARTATE

Ratio 1	Median	Ratio 2	Median	Difference	95% CI	*P**
^{68}Ga-DOTATATE to liver (1 h)	3.92	^{64}Cu-SARTATE to liver (1 h)	5.45	1.35	0.7, 2.2	0.004
^{68}Ga-DOTATATE to liver (1 h)	3.92	^{64}Cu-SARTATE to liver (4 h)	6.70	3.86	1.5, 6.4	0.002
^{64}Cu-SARTATE to liver (4 h)	6.70	^{64}Cu-SARTATE to liver (24 h)	16.69	6.75	3.4, 10.3	0.002

*Paired Wilcoxon test on 10 patients.
CI = confidence interval.

Comparison of Same-Day ^{68}Ga-DOTATATE and ^{64}Cu-SARTATE Images

A comparison of the baseline ^{68}Ga-DOTATATE and serial ^{64}Cu-SARTATE images in all patients is displayed in Figure 2 using an upper threshold SUV of 20. The quality of images obtained at 1 h with ^{64}Cu-SARTATE was judged to be comparable to that of images obtained using ^{68}Ga-DOTATATE in 9 of 10 patients. One patient had superior definition of small liver lesions on ^{68}Ga-DOTATATE, which was judged as being diagnostically superior by 2 of 3 masked readers. However, the 4-h image in this patient was felt to be comparable to—and the 24-h ^{64}Cu-SARTATE was judged by all readers to be superior to—the ^{68}Ga-DOTATATE PET/CT obtained at 1 h. The SUV_{max} of the most intense lesion and mean of up to 5 reference lesions selected on the basis of baseline ^{68}Ga-DOTATATE (median, 4 lesions; mean, 3.3 lesions; range, 1–5 lesions) for each individual patient were significantly lower for ^{68}Ga-DOTATATE than for ^{64}Cu-SARTATE at both 1 h and 4 h (Table 3). Although the SUV_{max} of lesions did not change significantly on ^{64}Cu-SARTATE between 4 and 24 h, the progressive increase in lesion-to-liver ratio suggests that delayed imaging would provide optimal lesion detection (Table 4). Figure 3 provides an example of improved lesion detection on late imaging.

Delayed Image Quality

Image quality remained high at 24 h after administration of ^{64}Cu-SARTATE (Fig. 2). The delayed images demonstrated clearance of activity from the liver relative to tumor resulting in qualitatively improved image quality. This finding reflected primarily washout of liver activity, as the median SUV_{max} of lesions at 24 h was not significantly different from that at 4 h (34.8 vs. 33.3, $P = 0.16$).

Radiation Dosimetry

Dose estimates for major organs are presented in Table 5. The mean effective dose was 8.7 ± 1.6 mSv per administration (mean injected activity, 192 MBq) or 0.0454 mSv/MBq. Accordingly, an administered activity of 200 MBq would give an effective whole-body dose of approximately 9 mSv plus that related to the CT component of the study.

DISCUSSION

There is increasing evidence that changing either the radionuclide or the chelating agent can alter the affinity of SSAs for somatostatin receptors (*20*). Accordingly, the performance of novel radiopharmaceuticals cannot be reliably predicted by the receptor-binding affinity of the peptide (*21*). Additionally, when a long-lived radioisotope is used, retention of activity at sites of disease is important both for diagnostic and for therapeutic purposes. The radionuclides ^{64}Cu and ^{67}Cu are an attractive theranostic pair. The main advantages of ^{64}Cu as a diagnostic agent are its favorable positron energy, cyclotron production, and a half-life that enables both distribution to sites without on-site radiochemistry and delayed imaging after administration to patients (*22*). Imaging of tissue clearance kinetics will aid prospective dosimetry calculations for its therapeutic pair, ^{67}Cu, which also has favorable physical decay characteristics (*14*). These include a β-energy that is similar to that of ^{177}Lu (580 keV vs. 497 keV) but with a significantly shorter half-life (2.58 d vs. 6.71 d), providing a higher dose-rate.

The first study to use ^{64}Cu to image neuroendocrine tumors was completed by Anderson et al. in 2001 (*23*). Eight subjects with a history of neuroendocrine tumors were imaged by conventional scintigraphy with ^{111}In-pentetreotide, followed by PET imaging with ^{64}Cu-TETA-octreotide. PET images were collected at times ranging from 0 to 36 h after injection. Although a formal analysis of temporal changes in tracer uptake in tumor deposits was not performed, the authors noted that lesions were more clearly visualized on the early images than on the delayed images and that the best imaging time appeared to be approximately 4–6 h after tracer injection. A subsequent study completed by Pfeifer et al. (*24*), investigated the biodistribution and image quality of ^{64}Cu-DOTATATE in 14 subjects with histologically confirmed neuroendocrine tumors, again with comparison to ^{111}In-pentetreotide. PET/CT scans were acquired at 1, 3, and 24 h after administration. Compared with conventional scintigraphy, ^{64}Cu-DOTATATE PET/CT identified additional lesions

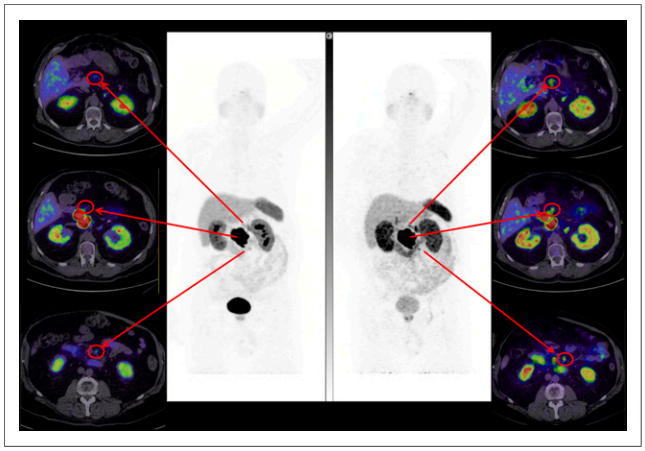

FIGURE 3. Superior lesion detection at 4 h. High lesion contrast on ^{64}Cu-SARTATE images at 4 h (right) better defines regional nodal disease than ^{68}Ga-DOTATATE images at 1 h (left) in patient with large pancreatic primary tumor but slightly greater small-bowel activity, indicating some hepatobiliary excretion.

TABLE 5
Absorbed Organ Doses in Comparison with ^{64}Cu-DOTATATE Data of Pfeifer et al. (*24*)

Organ	Patient 1	Patient 2	Patient 3	Patient 4	Patient 5	Patient 6	Patient 7	Patient 8	Patient 9	Patient 10	Mean	SD	Pfeifer mean
Adrenals	4.14E−01	1.81E−01	4.88E−02	1.96E−01	8.19E−02	5.67E−02	3.18E−02	2.36E−01	1.55E−01	2.91E−01	1.69E−01	1.22E−01	1.37E−01
Brain	1.53E−02	1.48E−02	2.19E−02	1.43E−02	9.45E−03	1.51E−02	1.39E−02	1.03E−02	1.20E−02	1.15E−02	1.39E−02	3.50E−03	1.27E−02
Breasts	1.38E−02	1.37E−02	2.07E−02	1.18E−02	8.86E−03	1.33E−02	1.18E−02	9.68E−03	1.09E−02	1.08E−02	1.25E−02	3.31E−03	1.32E−02
Gallbladder wall	2.78E−02	2.79E−02	3.60E−02	2.33E−02	1.91E−02	2.43E−02	2.36E−02	1.94E−02	2.14E−02	2.14E−02	2.44E−02	5.06E−03	3.96E−02
LLI wall	6.47E−02	3.24E−02	6.74E−02	7.06E−02	3.29E−02	4.44E−02	5.68E−02	2.90E−02	3.13E−02	5.35E−02	4.83E−02	1.63E−02	4.32E−02
Small intestine	6.83E−02	5.53E−02	7.92E−02	8.36E−02	5.83E−02	8.59E−02	9.53E−02	6.16E−02	4.98E−02	6.88E−02	7.06E−02	1.49E−02	6.55E−02
Stomach wall	6.92E−02	5.43E−02	3.85E−02	3.61E−02	4.13E−02	3.62E−02	2.58E−02	2.19E−02	4.87E−02	7.50E−02	4.47E−02	1.73E−02	1.93E−02
ULI wall	5.33E−02	5.55E−02	7.02E−02	3.91E−02	4.39E−02	1.24E−01	7.74E−02	4.79E−02	5.37E−02	5.92E−02	6.24E−02	2.45E−02	2.18E−02
Heart wall	2.66E−02	2.65E−02	3.69E−02	1.92E−02	1.62E−02	2.11E−02	2.33E−02	1.68E−02	2.98E−02	2.02E−02	2.37E−02	6.41E−03	1.86E−02
Kidneys	1.48E−01	1.88E−01	2.76E−01	2.20E−01	1.87E−01	2.42E−01	2.10E−01	1.82E−01	1.97E−01	1.73E−01	2.02E−01	3.66E−02	1.39E−01
Liver	1.20E−01	1.21E−01	1.14E−01	8.15E−02	8.14E−02	5.21E−02	7.88E−02	7.01E−02	7.56E−02	7.22E−02	8.67E−02	2.34E−02	1.61E−01
Lungs	2.75E−02	2.60E−02	2.89E−02	2.10E−02	1.71E−02	2.30E−02	2.39E−02	1.92E−02	2.03E−02	2.00E−02	2.27E−02	3.85E−03	1.67E−02
Muscle	1.68E−02	1.63E−02	2.43E−02	1.48E−02	1.10E−02	1.71E−02	1.50E−02	1.20E−02	1.37E−02	1.36E−02	1.55E−02	3.70E−03	1.90E−02
Ovaries	2.13E−02	1.96E−02	3.03E−02	2.07E−02	1.44E−02	2.44E−02	2.07E−02	1.53E−02	1.64E−02	1.79E−02	2.01E−02	4.68E−03	1.92E−02
Pancreas	9.40E−02	1.89E−01	7.24E−02	9.91E−02	4.48E−02	8.65E−02	6.95E−02	6.85E−02	1.05E−01	7.01E−02	8.99E−02	3.91E−02	9.27E−02
Red marrow	4.87E−02	3.99E−02	6.23E−02	5.03E−02	3.23E−02	4.12E−02	4.34E−02	3.40E−02	4.47E−02	3.74E−02	4.34E−02	8.82E−03	2.65E−02
Osteogenic cells	4.76E−02	4.26E−02	6.74E−02	4.57E−02	3.09E−02	4.36E−02	4.16E−02	3.31E−02	4.05E−02	3.69E−02	4.30E−02	1.01E−02	3.35E−02
Skin	1.29E−02	1.28E−02	1.98E−02	1.14E−02	8.36E−03	1.30E−02	1.12E−02	9.16E−03	1.02E−02	1.03E−02	1.19E−02	3.19E−03	1.22E−02
Spleen	2.47E−01	3.05E−01	3.33E−01	2.01E−01	2.64E−01	2.55E−01	3.97E−01	5.96E−01	6.20E−01	3.92E−01	3.61E−01	1.44E−01	1.15E−01
Testes	1.41E−02	1.38E−02	2.18E−02	1.30E−02	9.04E−03	1.55E−02	1.24E−02	9.78E−03	1.09E−02	1.13E−02	1.31E−02	3.64E−03	1.36E−02
Thymus	1.55E−02	1.53E−02	2.34E−02	1.33E−02	9.84E−03	1.49E−02	1.33E−02	1.07E−02	1.25E−02	1.21E−02	1.41E−02	3.77E−03	1.49E−02
Thyroid	5.24E−02	3.68E−02	8.06E−02	2.29E−02	1.98E−02	5.25E−02	4.32E−02	2.01E−02	3.72E−02	2.41E−02	3.90E−02	1.92E−02	1.41E−02
UB wall	6.73E−02	6.03E−02	7.66E−02	1.27E−01	5.59E−02	2.16E−01	7.38E−02	4.91E−02	5.30E−02	6.61E−02	8.46E−02	5.13E−02	3.70E−02
Uterus	2.05E−02	1.93E−02	2.95E−02	2.08E−02	1.41E−02	2.56E−02	1.98E−02	1.49E−02	1.60E−02	1.73E−02	1.98E−02	4.81E−03	1.89E−02
Total body	2.22E−02	2.17E−02	3.01E−02	1.97E−02	1.53E−02	2.10E−02	2.00E−02	1.68E−02	1.88E−02	1.80E−02	2.04E−02	4.06E−03	2.50E−02

LLI = lower large intestine; ULI = upper large intestine; UB = urinary bladder.
Data are mGy/MBq.

in 6 of 14 (43%) patients. However, the images presented in this paper also suggest poor visualization of lesions at 24 h. A more recent paper from the same group compared ^{64}Cu-DOTATATE PET/CT to ^{111}In-pentetreotide SPECT/CT in 111 patients but imaged patients with the PET tracer only at 1 h after tracer administration (*25*). Although this emulates the time at which ^{68}Ga tracers are typically imaged, it does not leverage the potential advantages of the longer half-life of ^{64}Cu. To our knowledge, no direct comparison of ^{64}Cu-DOTATATE and ^{68}Ga-DOTATATE in humans has been reported.

As well as assessing its safety, this first-time-in-humans study was designed to assess whether the high binding-affinity of the MeCOSar chelating agent for ^{64}Cu observed in murine models (*15*) is reproduced in humans. Supporting the preclinical promise of this agent, there was high retention in tumor deposits and substantial hepatic clearance leading to a significant increase in lesion contrast in the liver, as well as excellent ongoing visualization of extrahepatic disease. Image quality and SUV analysis suggests that, for the patient convenience of same-day imaging, acquisition at 4 h would be optimal, although earlier imaging is feasible, being comparable with ^{68}Ga-DOTATATE PET/CT in most (9/10) patients. Although less convenient for patients, delayed imaging at 24 h is also feasible, with particularly high lesion-to-liver contrast at this time, potentially improving the sensitivity of detection of disease in this organ, which is a major site of metastases in NEN (*26*).

Since all patients were selected on the basis of a positive ^{68}Ga-DOTATATE scan, the utility of ^{64}Cu-SARTATE in patients with low or absent tumor uptake on ^{68}Ga-DOTATATE PET/CT could not be assessed. Another potential limitation is that ^{68}Ga-DOTATATE PET/CT always preceded the ^{64}Cu-SARTATE study. However, reference lesions were all first defined on the ^{68}Ga-DOTATATE study and were the most intense lesions on this scan. Accordingly, the likelihood of partial-volume effects was low on the initial scan and, given selection of G1–G2 patients, the likelihood that significant growth through the partial-volume count recovery curve accounts for the increased lesion visualization is low with a mean delay of only 14 d between the scans.

No significant adverse events were seen with ^{64}Cu-SARTATE administration. The transient minor reduction in lymphocyte and leukocyte counts in 2 patients did not appear to be related to radiation dose to either the spleen or the red marrow, which were similar to those in other patients. This reduction may represent a normal fluctuation in these counts, given that both patients had counts that were otherwise persistently in the lower end of the reference range, in one case probably related to prior radionuclide therapy. We do not consider these findings likely to affect the suitability of this peptide as a therapeutic agent. The effective whole-body radiation dose was approximately 9 mSv for a 200-MBq (0.0454 mSv/MBq) administered activity. This estimate is in keeping with the long physical half-life and per-decay energy emission of ^{64}Cu relative to other PET isotopes, as well as previous dose reports for ^{64}Cu-DOTATATE by Pfeifer et al. (0.0315 mSv/MBq) (*24*). Organ doses were also comparable to the Pfeifer publication, although kidney and spleen doses were higher as indicated by the SUV data. These slight differences between dosimetry data may be related to the biologic affinity of SARTATE versus DOTATATE molecules for somatostatin receptor-2 and altered clearance from normal organs.

CONCLUSION

High uptake and retention of ^{64}Cu-SARTATE in tumors and accompanying clearance of activity from the liver provides high-contrast diagnostic images until at least 24 h after injection, increasing the flexibility for timing of diagnostic imaging and the potential for multiple time-point dosimetry estimation before ^{67}Cu-SARTATE PRRT. The longer half-life of ^{64}Cu than of ^{68}Ga also makes the former agent suitable for commercial good-manufacturing-practice production and distribution to remote sites. This preliminary evaluation indicates that the agent is safe and has acceptable radiation dosimetry for human use as a diagnostic agent, with improved imaging characteristics at 4 h compared with 1 h.

DISCLOSURE

This study was funded by Clarity Pharmaceuticals. Rodney Hicks is the recipient of a National Health and Medical Research Council Practitioner Fellowship (APP1108050), which supported this work. Amos Hedt and Matthew Harris are employed by Clarity Pharmaceuticals, the licensee of the intellectual property for SARTATE. Charmaine Jeffery has Clarity Pharmaceuticals share options. Paul Donnelly and Brett Paterson are inventors of, and hold intellectual property in, this area of research, which has been licensed from the University of Melbourne to Clarity Pharmaceuticals. Brett Paterson and Paul Donnelly possess share options in Clarity Pharmaceuticals. Paul Donnelly serves on the Scientific Advisory Board of Clarity Pharmaceuticals. Unrelated to this project, Rodney Hicks has share options in Telix Radiopharmaceuticals that are held on behalf of the Peter MacCallum Cancer Centre. No other potential conflict of interest relevant to this article was reported.

ACKNOWLEDGMENTS

We thank the patients for participating in the study and the Molecular Imaging Team and Neuroendocrine Tumour Service for diligently performing excellent work.

REFERENCES

1. Deppen SA, Blume J, Bobbey AJ, et al. ^{68}Ga-DOTATATE compared with ^{111}In-DTPA-octreotide and conventional imaging for pulmonary and gastroenteropancreatic neuroendocrine tumors: a systematic review and meta-analysis. *J Nucl Med.* 2016;57:872–878.
2. Hicks RJ. Use of molecular targeted agents for the diagnosis, staging and therapy of neuroendocrine malignancy. *Cancer Imaging.* 2010;10(spec no A):S83–S91.
3. Kwekkeboom DJ, de Herder WW, van Eijck CH, et al. Peptide receptor radionuclide therapy in patients with gastroenteropancreatic neuroendocrine tumors. *Semin Nucl Med.* 2010;40:78–88.
4. Hofman MS, Hicks RJ. Changing paradigms with molecular imaging of neuroendocrine tumors. *Discov Med.* 2012;14:71–81.
5. Bodei L, Cremonesi M, Ferrari M, et al. Long-term evaluation of renal toxicity after peptide receptor radionuclide therapy with ^{90}Y-DOTATOC and ^{177}Lu-DOTATATE: the role of associated risk factors. *Eur J Nucl Med Mol Imaging.* 2008;35:1847–1856.
6. Kashyap R, Jackson P, Hofman MS, et al. Rapid blood clearance and lack of long-term renal toxicity of ^{177}Lu-DOTATATE enables shortening of renoprotective amino acid infusion. *Eur J Nucl Med Mol Imaging.* 2013;40:1853–1860.
7. Sabet A, Ezziddin K, Pape UF, et al. Accurate assessment of long-term nephrotoxicity after peptide receptor radionuclide therapy with ^{177}Lu-octreotate. *Eur J Nucl Med Mol Imaging.* 2014;41:505–510.
8. Beauregard J-M, Hofman MS, Pereira JM, Eu P, Hicks RJ. Quantitative ^{177}Lu SPECT (QSPECT) imaging using a commercially available SPECT/CT system. *Cancer Imaging.* 2011;11:56–66.
9. Hicks RJ, Kwekkeboom DJ, Krenning E, et al. ENETS consensus guidelines for the standards of care in neuroendocrine neoplasia: peptide receptor radionuclide therapy with radiolabeled somatostatin analogues. *Neuroendocrinology.* 2017;105:295–309.

10. Strosberg J, El-Haddad G, Wolin E, et al. Phase 3 trial of ^{177}Lu-dotatate for midgut neuroendocrine tumors. *N Engl J Med.* 2017;376:125–135.
11. Hofman MS, Hicks RJ. Peptide receptor radionuclide therapy for neuroendocrine tumours: standardized and randomized, or personalized? *Eur J Nucl Med Mol Imaging.* 2014;41:211–213.
12. Beauregard JM, Hofman MS, Kong G, Hicks RJ. The tumour sink effect on the biodistribution of ^{68}Ga-DOTA-octreotate: implications for peptide receptor radionuclide therapy. *Eur J Nucl Med Mol Imaging.* 2012;39:50–56.
13. Pauwels S, Barone R, Walrand S, et al. Practical dosimetry of peptide receptor radionuclide therapy with ^{90}Y-labeled somatostatin analogs. *J Nucl Med.* 2005;46(suppl 1):92S–98S.
14. Novak-Hofer I, Schubiger PA. Copper-67 as a therapeutic nuclide for radioimmunotherapy. *Eur J Nucl Med Mol Imaging.* 2002;29:821–830.
15. Paterson BM, Roselt P, Denoyer D, et al. PET imaging of tumours with a ^{64}Cu labeled macrobicyclic cage amine ligand tethered to Tyr^3-octreotate. *Dalton Trans.* 2014;43:1386–1396.
16. Frilling A, Clift AK. Therapeutic strategies for neuroendocrine liver metastases. *Cancer.* 2015;121:1172–1186.
17. Klein S, Staring M, Murphy K, Viergever MA, Pluim JP. Elastix: a toolbox for intensity-based medical image registration. *IEEE Trans Med Imaging.* 2010;29:196–205.
18. Jackson PA, Beauregard J-M, Hofman MS, Kron T, Hogg A, Hicks RJ. An automated voxelized dosimetry tool for radionuclide therapy based on serial quantitative SPECT/CT imaging. *Med Phys.* 2013;40:112503.
19. Stabin MG, Sparks RB, Crowe E. OLINDA/EXM: the second-generation personal computer software for internal dose assessment in nuclear medicine. *J Nucl Med.* 2005;46:1023–1027.
20. Fani M, Del Pozzo L, Abiraj K, et al. PET of somatostatin receptor-positive tumors using ^{64}Cu- and ^{68}Ga-somatostatin antagonists: the chelate makes the difference. *J Nucl Med.* 2011;52:1110–1118.
21. Hicks RJ. Citius, Altius, Fortius: an Olympian dream for theranostics. *J Nucl Med.* 2017;58:194–195.
22. Williams HA, Robinson S, Julyan P, Zweit J, Hastings D. A comparison of PET imaging characteristics of various copper radioisotopes. *Eur J Nucl Med Mol Imaging.* 2005;32:1473–1480.
23. Anderson CJ, Dehdashti F, Cutler PD, et al. ^{64}Cu-TETA-octreotide as a PET imaging agent for patients with neuroendocrine tumors. *J Nucl Med.* 2001;42:213–221.
24. Pfeifer A, Knigge U, Mortensen J, et al. Clinical PET of neuroendocrine tumors using ^{64}Cu-DOTATATE: first-in-humans study. *J Nucl Med.* 2012;53:1207–1215.
25. Pfeifer A, Knigge U, Binderup T, et al. ^{64}Cu-DOTATATE PET for neuroendocrine tumors: a prospective head-to-head comparison with ^{111}In-DTPA-octreotide in 112 patients. *J Nucl Med.* 2015;56:847–854.
26. Frilling A, Modlin IM, Kidd M, et al. Recommendations for management of patients with neuroendocrine liver metastases. *Lancet Oncol.* 2014;15:e8–e21.